Interfacial Crack Arrest in Sandwich Panels with Embedded Crack Stoppers Subjected to Fatigue Loading

Martakos, G.; Andreasen, J. H.; Berggreen, Christian; Thomsen, O. T.

Published in:
Applied Composite Materials

Link to article, DOI:
10.1007/s10443-016-9514-3

Publication date:
2017

Document Version
Peer reviewed version

Applied Composite Materials

Interfacial Crack Arrest in Sandwich Panels with Embedded Crack Stoppers Subjected to Fatigue Loading

--Manuscript Draft--

Manuscript Number:	ACMA-D-16-00317R1
Full Title:	Interfacial Crack Arrest in Sandwich Panels with Embedded Crack Stoppers Subjected to Fatigue Loading
Article Type:	Original Research
Keywords:	Sandwich structures, Composites, Finite Element Analysis, Fracture mechanics, Fatigue
Corresponding Author:	Georgios Martakos, MSc Aalborg University Aalborg, DENMARK
Corresponding Author Secondary Information:	
Corresponding Author's Institution:	Aalborg University
Corresponding Author's Secondary Institution:	
First Author:	Georgios Martakos, MSc
First Author Secondary Information:	
Order of Authors:	Georgios Martakos, MSc
	Jens Henrik Andreasen
	Christian Berggreen
	Ole Thybo Thomsen
Order of Authors Secondary Information:	
Funding Information:	
Abstract:	A novel crack arresting device has been implemented in sandwich panels and tested using a special rig to apply out-of-plane loading on the sandwich panel face-sheets. Fatigue crack propagation was induced in the face-core interface of the sandwich panels which met the crack arrester. The effect of the embedded crack arresters was evaluated in terms of the achieved enhancement of the damage tolerance of the tested sandwich panels. A finite element (FE) model of the experimental setup was used for predicting propagation rates and direction of the crack growth. The FE simulation was based on the adoption of linear fracture mechanics and a fatigue propagation law (i.e. Paris law) to predict the residual fatigue life-time and behaviour of the test specimens. Finally, a comparison between the experimental results and the numerical simulations was made to validate the numerical predictions as well as the overall performance of the crack arresters.
Response to Reviewers:	Dear Dr. Beaumont, Thank you for your commments and suggestions. I have revised the mauscript as you suggested and have resubmitted it. Best regards, Georgios Martakos

Interfacial Crack Arrest in Sandwich Panels with Embedded Crack Stoppers Subjected to Fatigue Loading

G. Martakos[1], J.H. Andreasen[1], C. Berggreen[2], O.T. Thomsen[3,1]

[s1]Department of Mechanical and Manufacturing Engineering, Aalborg University

Fibigerstræde 16, DK-9220 Aalborg East, Denmark

Email: {gm,jha, ott}@m-tech.aau.dk, web page: http://www.m-tech.aau.dk

[3]Department of Mechanical Engineering, Technical University of Denmark

Nils Koppels Allé, Building 403, DK-2800 Kgs. Lyngby, Denmark

Email: cbe@mek.dtu.dk, web page: http://www.dtu.dk

[3]Faculty of Engineering and the Environment,
University of Southampton, Highfield, Southampton, UK

Email: o.thomsen@soton.ac.uk , web page: http://www.soton.ac.uk/engineering/

Keywords: Sandwich structures, Composites, Finite Element Analysis, Fracture mechanics, Fatigue

ABSTRACT:

A novel crack arresting device has been implemented in sandwich panels and tested using a special rig to apply out-of-plane loading on the sandwich panel face-sheets. Fatigue crack propagation was induced in the face-core interface of the sandwich panels which met the crack arrester. The effect of the embedded crack arresters was evaluated in terms of the achieved enhancement of the damage tolerance of the tested sandwich panels. A finite element (FE) model of the experimental setup was used for predicting propagation rates and direction of the crack growth. The FE simulation was based on the adoption of linear fracture mechanics and a fatigue propagation law (i.e. Paris law) to predict the residual fatigue life-time and behaviour of the test specimens. Finally, a comparison between the experimental results and the numerical simulations was made to validate the numerical predictions as well as the overall performance of the crack arresters.

1. INTRODUCTION

Sandwich structures represent a special form of laminated composites comprising stiff and thin face-sheets separated by and bonded to either side of a light and compliant core material. The resulting layered sandwich element or structure displays very high stiffness and strength to weight ratios [1,2]. Their structural attributes and the need for larger and ever lighter structures has led to the implementation of sandwich structures into many areas of industrial production, including aerospace, ship/marine, automotive and wind turbine blade structures to mention a few. Due to their extensive and increasing use, novel ways to further enhance the performance of sandwich structures are being pursued continuously. Consequently the wish to fully understand the behaviour of sandwich structures is increasing, as well as the need to control and predict the effect of limitations and weaknesses inherent in their nature. One of the main limitations of sandwich structures is their sensitivity to separation or debonding between the core material and the face-sheets. Moreover, debonds or dry spots can be introduced during manufacturing, especially for larger parts. The separated or debonded zones effectively act as inherent structural weak points/zones, which may lead to premature fracture in the core which is likely to develop into cracks separating the core and face-sheets. Such debonds may

progressively expand under the action of external loading (quasi-static of fatigue), and may lead to a global failure that occur with little or no prior warning.

The increasing interest concerning interfacial debond behaviour of sandwich components and structures has led to several studies including analytical, experimental and numerical approaches. Interfacial debonds can be considered and studied within the framework of fracture mechanics, since the conditions of debond progression and arrest can conveniently be described in terms of physical quantities defined through fracture mechanics. Several studies have discussed and applied the theoretical background for this [3-8] in describing bi-material and interface crack behaviour [3-6] and the conditions for crack kinking out of an interface [7-8]. However, it is only in the most recent studies that numerical tools have been successfully utilized to simulate interfacial crack growth in sandwich panels. Several methods have been proposed based on the Finite Element Method framework and have been used to simulate interface crack propagation convincingly. Recent examples include the Virtual Crack Closing Technique (VCCT) [9], the Crack Surface Displacement Extrapolation method (CSDE) [10-11] as well as cohesive zone modelling (CZM) [12]. Moreover, the CSDE method has been applied in conjunction with the cycle jump technique (CJT) [13-15] to reduce the calculated loading cycles of fatigue simulations. The mentioned methodologies have been applied for the simulation of interface fatigue crack growth in both sandwich beams and sandwich panels [15].

In this study the CSDE and CJT methods have been used to predict the interface crack propagation behaviour in foam cored sandwich panels with composite face-sheets. In addition, this study considers the conditions under which an embedded crack stopper device (in the form of a core insert) can promote crack deflection away from the face-sheet/core interface and into the sandwich core material following a pre-described propagation path along an interface between the crack stopper and the foam core material.

Previous attempts to delay or arrest propagating interfacial face-sheet core cracks by the use of special embedded crack stopping inserts (or devices) have been reported. In [16] two types of carbon fibre reinforced composite (CFRP) inserts loaded using the Sandwich Cantilever Beam (SCB) and Cracked Sandwich Specimen (CSB) tests were introduced to examine crack arrest under mode I and mode II loadings, respectively. It was shown that the embedded crack stopper devices/elements could arrest a propagating interface crack for a considerable amount of loading cycles, especially under mode II loading conditions. The reason for this effect is the much higher fracture toughness of the CFRP compared to conventional core materials as well as the geometry of the CFRP crack arresters. In [17-18] it was demonstrated that crack arrest can be achieved by using either a semi-circular CFRP rod glued onto face-sheet/core interface, or by using a splice-type crack arrester connecting the two face-sheets through CFRP layers. In both cases a stress release at the crack tip was observed as the crack approached the tip of the arresters. The reduction of stresses at the crack tip resulted in a reduction of the energy release rate and a deceleration of the crack. Finally, in [19-25] a new type of crack arrester (referred to as a peel stopper) was tested. The peel stopper, which is configured as a core insert made from a compliant/soft material bonded to both the face-sheets and sandwich core, is capable of re-directing propagating cracks away from the interface and subsequently arresting the cracks in the centre of the peel stopper. The peel stopper has been shown to be able to deflect and arrest propagating interface cracks in sandwich beams subjected to both quasi-static and fatigue loading conditions, and where the stress field near the crack trip is Mode II dominated [21, 25].

Following on from and inspired by the work presented in [26-28], a new and significantly lighter design of the peel stopper was proposed and implemented in sandwich beams [26-28]. Initially, the conditions under which the novel peel stopper was able to deflect a propagating face-sheet/core interface crack were investigated in [26]. This included testing of sandwich beams made of glass reinforced composite face-sheets (GFRP) and PVC foam core with embedded peel stoppers subjected to fatigue loads using the Mixed Mode Bending test (MMB) [26]. Three design variations of the peel stopper were tested showing that a design with glass fibres extruding from the tip of the peel stopper and extending into either the face-sheets or the face-sheet/core interface improved the interface crack deflection capabilities. The new peel stopper was further tested in sandwich beams using the Sandwich Tear Test (STT) in [27]. The aim of the research presented in [27, 28] was to evaluate and validate the ability of the new lightweight peel stopper design to delay or hinder interface crack propagation, and ultimately achieving crack arrest in composite foam cored sandwich beams subjected to fatigue loading conditions. This was achieved and the underlying physical mechanisms were accounted for

using both experimental and numerical approaches. It was further shown that the novel peel stopper design was capable of more than doubling the expected life time of sandwich beams.

This study concerns the fatigue testing of sandwich panels with GFRP face-sheet and PVC foam core that have been fitted with embedded peel stoppers of the improved design introduced in [26, 27, 28]. The ability of the peel stoppers to enhance the damage tolerance of sandwich panels, i.e. to delay or prevent interface crack propagation, has been investigated using both experimental observations and finite element (FE) analyses.

2. METHODS

2.1. Specimens/Materials

The experimental study involves testing of quadratic sandwich panels by applying transverse loads as a concentrated force applied through a metallic insert in the centre of the panel. To simplify the test rig design, it was chosen to use quadratic sandwich panels that are simply supported along all four edges. Fatigue loading was applied to progress a predefined face-sheet/core debond located in the centre of the panel around the loading point. Two types of sandwich panel specimens were manufactured; one with embedded peel stoppers and another without peel stoppers.

The peel stoppers were manufactured in a circular shape, and subsequently embedded in the sandwich foam core with the peel stopper circle having its centre coinciding with the sandwich panel centre. Thus the peel stopper is configured as a circular “barrier” around the load introduction area in the plate centre. The configuration with a central external load, and a concentric circular peel stopper was chosen to achieve a nearly axisymmetric strain and stress field in the vicinity of the plate centre and the peel stopper despite the fact that the sandwich panel specimens were in fact quadratic. The sandwich panel/plate dimensions were chosen such that edge effects from the four straight edges did not influence the strain and stress fields near the crack stopper.

Figure 1 shows the sandwich panel dimensions, the sandwich panel boundary and loading conditions, and the peel stopper shape and dimensions. The peel stopper cross section was designed with a double U shape, thus enabling crack deflection of face-sheet/core interface cracks propagating from the centre of the plate towards the edge as well as cracks propagating from the edge towards the centre (if that was to occur). Once deflected, cracks from both sides were allowed to propagate only until the middle of the peel stopper where the crack was arrested at the physical boundary created by the geometry of the peel stopper.

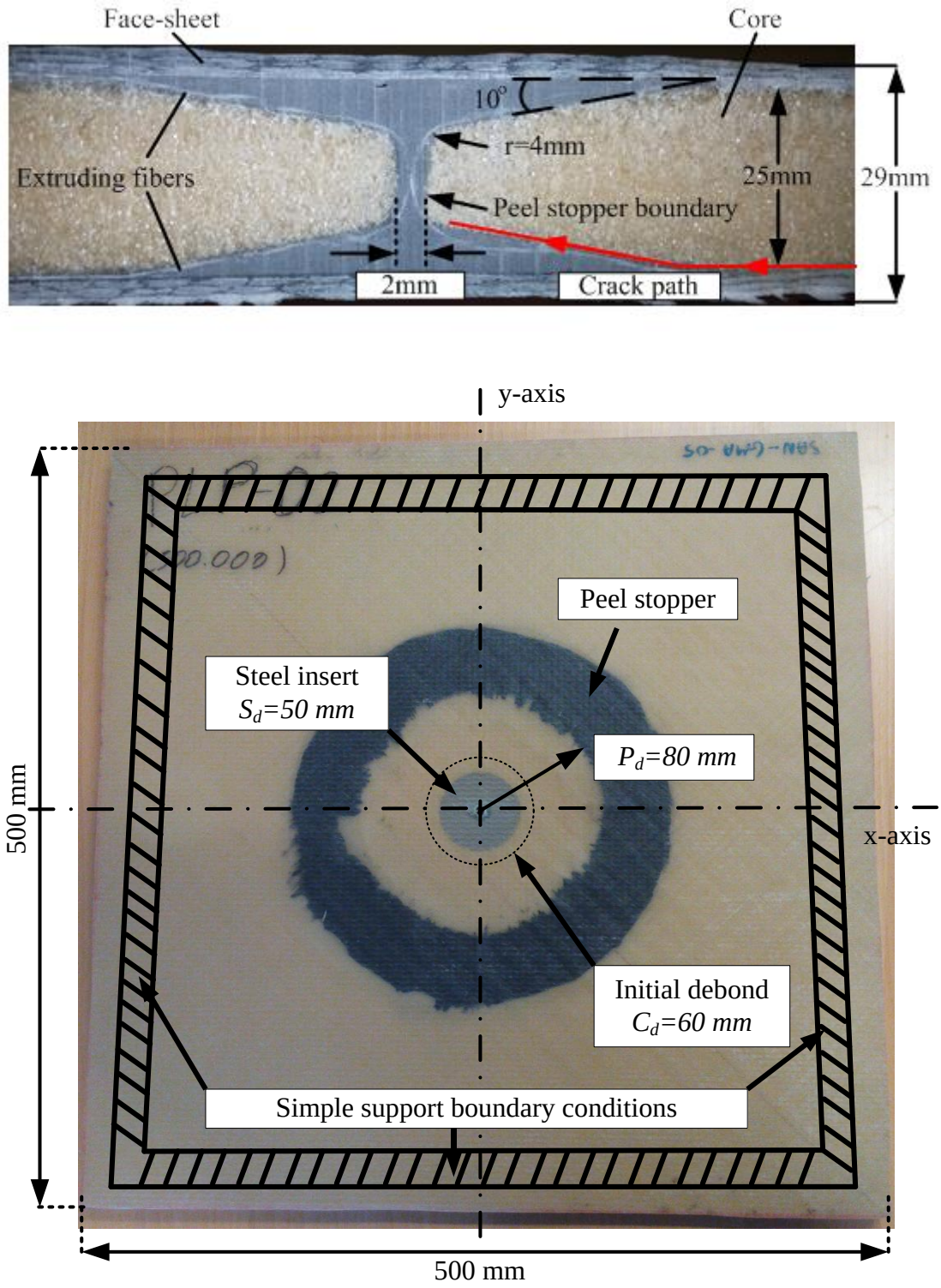

Figure 1. Layout and dimensions of foam cored sandwich panel test specimens with embedded PU peel stopper.

The peel stoppers were manufactured using a special mould tool made from Polypropylene. The peel stopper was made using a two-component Polyurethane (PU) resin (PERMALOCK 2K PU-9004) which was reinforced by UD glass fibres along its length as devised in [26]. The use of Polypropylene for the mould tool allowed easy de-moulding of the cast PU peel stoppers without the need of a release agent. For practical reasons the circular peel stopper configuration was made from 4 quarter circle sections that were manufactured separately and then embedded into the PVC foam core

material, see Figure 1. The glass reinforcement was first placed in the mould tool, and to reduce complexity during fabrication, the glass reinforcement was only extending from the side of the double U peel stopper shape (see Figure 1) facing towards the plate/panel centre. After this the PU resin was carefully poured into the mould tool, and subsequently the mould tool was closed to form the PU peel stopper. The PU peel stoppers were cured for 8 hours at room temperature.

The face-sheets of the sandwich panels consisted of 3 layers of glass reinforcement, quad-mat [0°/45°/90°/-45°] AMT (DBLT-850) from Devold, providing 2 mm thick face-sheets after the resin infusion. The resin system used was Huntsman Araldite LY 1564 SP/Hardener XB 3486. Divinycell H100 PVC foam from DIAB having a nominal density of 100 kg/m^3 [29] was used as the core material. This combination of composite face-sheets and core material was chosen, as it was used for the research presented in [27,28], from which the interface crack propagation properties are available. Table 1 summarizes the material properties of the sandwich panel specimens.

The sandwich panel specimens were fabricated in two steps. In the first step, the core structure comprising of the machined PVC foam material and the PU peel stoppers was assembled, and in the second step the glass reinforcement of the top and bottom face-sheets and the sandwich core were laid up into the mould tool. Finally, the entire assembly was infused using Vacuum Assisted Resin Transfer Moulding (VARTM).

The manufacturing of the sandwich panels without embedded peel stoppers was straightforward, as it only required cutting of the PVC H100 foam into the square shape of the sandwich panel, followed by milling of the cylindrical cut-out in the plate centre where a steel insert of diameter 50 mm and the same height as the foam core was placed in the succeeding process step.

For the sandwich panels with embedded peel stoppers, an additional extra milling process was conducted to shape the PVC foam to allow the assembly with the PU peel stoppers. Since the peel stopper appears as a "through thickness" core insert, the "inner" and "outer" areas of the foam were separated after milling. After the foam was milled, all the parts were bonded together using an epoxy adhesive, Araldite 2000. The core parts were pressed together using clamps while the adhesive was allowed to cure for one day at room temperature. After this the cylindrical steel insert was inserted in the centre of the square shaped core assembly, thus providing a means to apply the external loading into the sandwich specimens. The central steel insert was coated by a thin layer of Teflon to prevent bonding to the adjacent core and face-sheet components in the resin infusion process. This was chosen to assure that the desired crack was always initiated in the lower face-sheet/core interface of the panel specimens. Before the resin infusion an extra layer of Teflon foil of diameter 60 mm (see Figure 1) was inserted at the top face-sheet/core interface to induce an initial concentric crack front in the sandwich panel specimens. Finally, after following all the steps outlined above, the sandwich panel specimens were infused and cured at room temperature for 24 hours, followed by a post curing at 80^{o}C for an extra 12 hour period.

Table 1. Material properties of sandwich panel specimens [26-28]

Materials	In-plane Young's modulus (E_x)	Through thickness Young's modulus (E_y)	Shear modulus (G_{xy})	Poisson's ratio (ν_{xy})
DIVINYCELL H100	56 MPa	128 MPa	32 MPa	0.3
E-glass/epoxy	18.6 GPa	9.2GPa	2.7 GPa	0.4
PU	100 MPa	100 MPa	34.2 MPa	0.45

2.2. Test set-up

The tests were conducted using a Schenck 400 kN servo-hydraulic test machine with an Instron 8800 controller. A 10 kN load cell was mounted in the machine to improve the load control accuracy during the tests. Figure 2 shows the testing set-up, including load application through a central insert and the square shaped steel test rig providing the simply supported boundary conditions imposed along the panel edges. As indicated in Figure 2, the sandwich panels were simply resting on the square shaped steel test rig, providing approximate simple support conditions along the four panel edges. Rubber strips were attached to the supporting flat steel surfaces of the test rig, and the specimens rested on these rubber strips to avoid indentation damage during testing. The test rig was mounted to the cross-head of the test machine, hanging from the load cell attached to the load frame of the test machine. The mounted test rig was placed as high as possible to maximize the distance between the hydraulic actuator at the bottom of the test frame and the underside of the panel specimen. This was done to maximize the viewing area of the 2 digital cameras facing upwards towards the panel specimens and used for digital image correlation (DIC) measurements. To apply the loads from the actuator to the specimen, an extension rod was attached to the actuator. The rod was made from aluminium with a diameter of 25 mm to minimize the obscuring of the field of view for the 2 digital cameras.

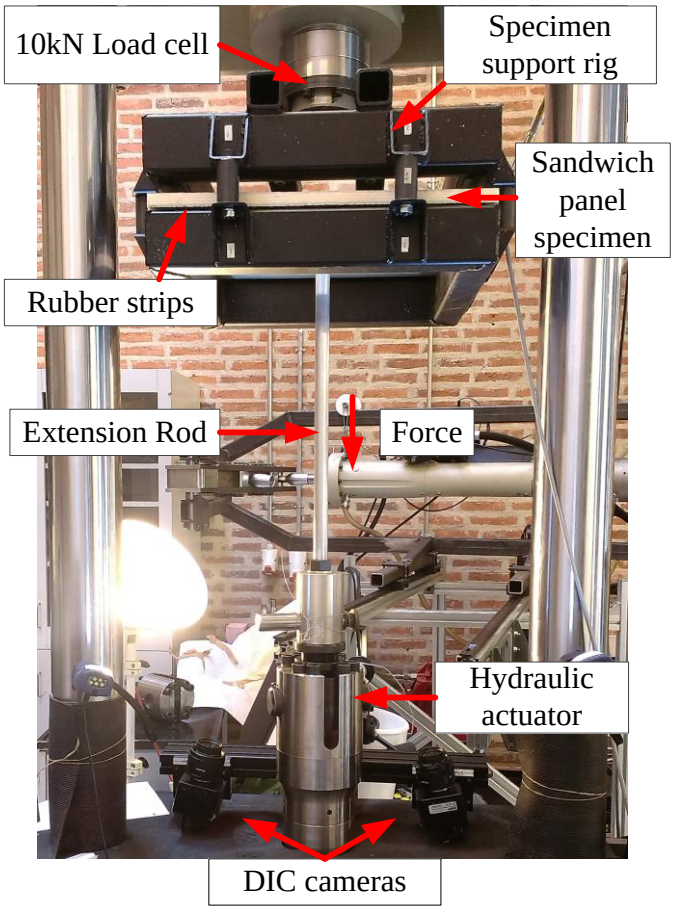

Figure 2. Sandwich panel testing setup and DIC setup of the tested sandwich panels.

As mentioned above, the sandwich panels were subjected to a central point load applied through the central loading insert. The test was designed to drive the face-sheet/core interface crack pre-initiated in the centre of the sandwich panels towards the peel stopper and outer panel boundary. The advantage of this test setup is that the interface crack propagation is both predictable and easy to control as the crack propagates steadily under all load control schemes. The central force loading applied to the specimens led to a sub-interface crack propagation path without any occurrence of crack kinking into the foam material, as the mode mixity induced always drove the crack to propagate towards the debonded face-sheet rather than into the core. In fact, the crack tended to propagate on the core side just below the facesheet/core interface, The self-similar crack propagation behaviour in all tested specimens allowed for a high

consistency and repeatability throughout the tests and thus reduced the number of test repetitions required. Three tests were conducted under load controlled fatigue loading conditions with an R-ratio of $R = 0.1$; two specimens with embedded peel stoppers, and one specimen without a peel stopper. In addition, one sandwich panel specimen was tested subject to quasi-static loading in order to derive the appropriate load amplitudes imposed in the fatigue tests. Figure 3 shows the force vs, cross-head displacement obtained from the quasi-static test, where the panel specimen was loaded in displacement control until the interface crack propagated two times before the test was stopped. The four sandwich panel specimens are presented in Table 2.

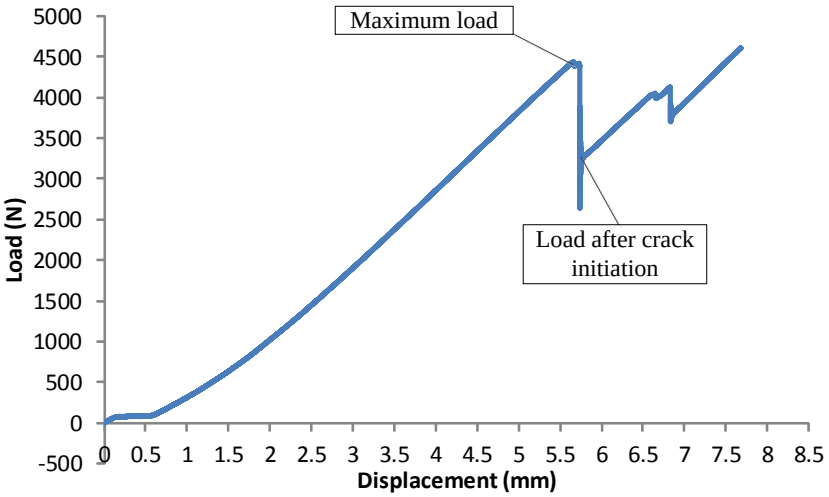

Figure 3. Load-displacement obtained from quasi-static testing of a sandwich panel without a peel stopper.

Table 2. Sandwich panel specimens used for fatigue and quasi-static load tests.

Specimen name	*Loading conditions*	*Specimen Type*
PLP 1	*Fatigue*	*with embedded peel stopper*
PLP 2	*Fatigue*	
PLT 1	*Quasi-static*	*Without peel stopper*
PLT 2	*Fatigue*	

The fatigue load applied to specimens PLT2 (without peel stopper) and PLP1, PLP2 (with embedded peel stoppers) was chosen to be about 80% of the maximum load obtained for PLT1 (quasi-static test), and equal to the load where interface crack propagation first occurred. As the interface crack front propagated from the centre of the panel, the load was distributed along a larger circumference as well as contributing to an increasing membrane force build-up in the debonded face-sheet, and thus the stresses as well as energy release rate at the crack tip reduced acordingly, with the important implication that the applied load amplitude needed to be increased to propagate the crack further. If the fatigue loading had been applied at a constant magnitude throughout the entire test, this would have resulted in a self arresting propagation mechanism, where the interface crack propagation would have deccelerated as the debonded interface crack area increased in size (diameter). Despite this fact, the fatigue load amplitude was chosen to remain contant throughout the entire test, since the initially chosen load amplitude was proven to be sufficiently high to propagate the crack far enough to assess the peel stopper performance.It is important to note here that the energy release rate of the crack is directly infuencing the performance of the peel stopper. Higher loads will effectively result in a reduced crack arrest time, while lower loads will enhance it. However, the effect of the load magnitude has been taken

out in this study by testing also specimens without peel stoppers. The evaluation is based on a comparison of the fatigue life of specimens with and without crack stoppers loaded under the same load ampitude.

Since visual identification of the crack position was impossible, the duration of the tests could not be controlled based on visual inspection. The number of cycles to test completion was selected based on DIC observations, which gave an indication of the crack position inside the panels. This procedure required testing of the sandwich panels up to an initialy selected number of cycles, followed by post-processing of the images captured by the DIC system to identify the crack position. In cases where the crack had not propagated adequately, the test was continued. Initially a total of 250.000 load cycles were imposed for all panels. For the case of the panel without a peel stopper the number of cycles was found to be sufficient to propagate the crack at a radius of approximetaly 100 mm without the need to increase load magnitud. For the two panels with embedded peel stoppers 250.000 cycles resulted in a crack propagation radius of 82 mm. This was found inadequate and an additional 250,000 loading cycles were imposed (thus reaching a total of 500,000 cycles for the 2 panels with embedded peel stoppers) to propagate the crack further. With the additional loading cycles the crack grew to a radius of approximetaly 85 mm. The experiements were terminated at this stage, as it was observed that the crack growth rate at the specified load magnitude was so low that further continuation would not result in a substantial increase of the crack radius. Table 3 summarizes the fatigue loading conditions applied to the 4 sandwich panel specimens.

Table 3. Fatigue loading configuration

Fatigue test data	*Fatigue load*
Fatigue maximum load	*3800 N*
Fatigue minimum load	*380 N*
Load Ratio	*0.1*
Frequency	*2 Hz*

2.3 Digital Image Correlation (DIC)

A two camera DIC system was used to capture the out-of-plane displacements of the lower face-sheet of the tested sandwich panels as the face/core debond propagated (see test setup in Figures 2 and 4). The DIC system used was an ARAMIS 4M system from GOM GmbH. The DIC software ARAMIS v6.2.0 was used to post-process and extract deformation data from the images. The digital cameras were placed below the specimen facing upwards at a distance of approximately 1 m from the sandwich specimen underside surface (lower face-sheet), see Figure 4. The observed area or the Region of Interest (RoI) covered an area of approximately 250 mm by 250 mm in the centre of the lower face-sheet, within the region of where the peel stoppers were positioned and the interface crack was expected to propagate. A random speckle pattern was sprayed onto the lower face-sheet covering the RoI. A thin strip of tape was placed on one side of the panel along the x-axis (see Figure 2). The strip created a thin line in the RoI, clear of the speckle pattern allowing the identification of the crack front location relative to the peel stopper, when the images were post-processed. This enabled the inspection of the crack front propagation radius which was used to control of the total duration of the tests, as explained in the previous section. Images of the RoI were automatically recorded every 60 seconds during the fatigue tests. The DIC setup and image processing details are given in table 4.

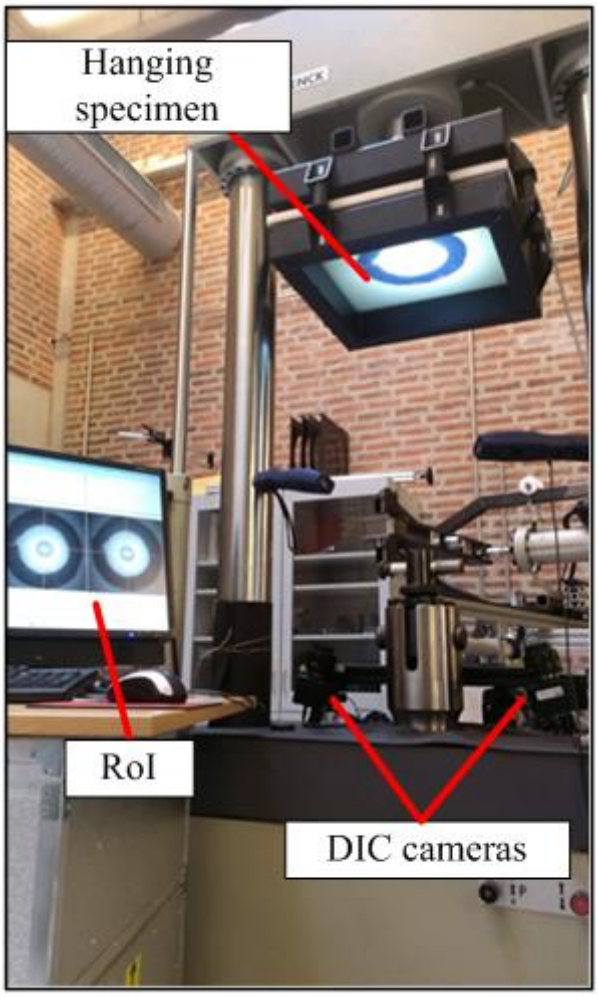

Figure 4. Dual camera DIC setup and Region of Interest (RoI) on the tested sandwich panels.

Table 4. Specification of DIC setup and processing

Technique used	*3D digital image correlation*
Subset size	*15×15 pixel²*
Shift	*15 pixel*
Cameras	*8 bit, 2048×2048 ARAMIS 4M system*
Field of view	*250×250 mm²*
Measurement points	*18769*
Displacement	
Spatial resolution	*1.83mm/15pixel*
Resolution	*122 μm*
Strain	
Smoothing method	*Gaussian Average (3×3)*
Differentiation method	*Finite differences*

3. NUMERICAL ANALYSES

A three dimensional (3D) Finite Element (FE) model was developed in the commercial software package ANSYS 15.0 [30]. The model was developed to simulate crack growth in the sandwich panel specimens with and without peel stoppers subjected to fatigue loading conditions. To capture the 3D nature of the problem, the crack propagation in the face-sheet/core and core/PU interfaces was modelled by means of a 3D crack front. By using the mesh at the crack tip, the CSDE mode-mixity method [10-11] was used to extract the energy release rate and mode-mixity along the crack tip front. Each nodal point was able to move independently in a direction perpendicular to the crack front depending on the energy release rate and mode-mixity values, respectively. By the use of a re-meshing algorithm, the 3D crack propagation inside the sandwich panels was simulated.

Figure 5 and 6 show the detailed 3D FE models for both the specimens with and without peel stoppers. Only one quarter of the sandwich plate specimens were modelled due to double-symmetry of the test specimens. The main panel model consisting of 8.000-14.000 20-node solid elements, depending on the radius of the crack front modelled. Geometrical non-linear analyses were conducted to accurately account for the large displacements and rotations of the debonded face-sheet during the experiments, as well as membrane effects in the debonded face-sheet.

It is observed from Figure 6 that the peel stopper was not modelled in great detail, and that only the lower part facing towards the panel centre was included in the model. The reason being that the geometric complexity of the peel stopper created meshing instability issues in the crack simulation analyses. The fatigue crack propagation is simulated by repeated loops of defining the new crack position and then re-meshing the model accordingly without user intervention. This means that high geometric complexity is bound to lead to occasional errors in meshing that would stop the simulations. To avoid this, the geometric complexity of the model had to be reduced significantly. The cause derives from the choice to use 20-node cubic elements to mesh the entire geometry of the model. ANSYS requires a very structured division of the model geometry to enable automatically meshing with 20-node elements without errors. To avoid meshing errors as the crack front propagated radially in the panel along the face-sheet/core and core/PU interfaces, the FE model was divided into volumes of more generic shapes. Since the crack propagation was modelled only in the face-sheet/core and core/PU interfaces, it was not necessary to develop a more detailed FE meshing of the peel stopper.

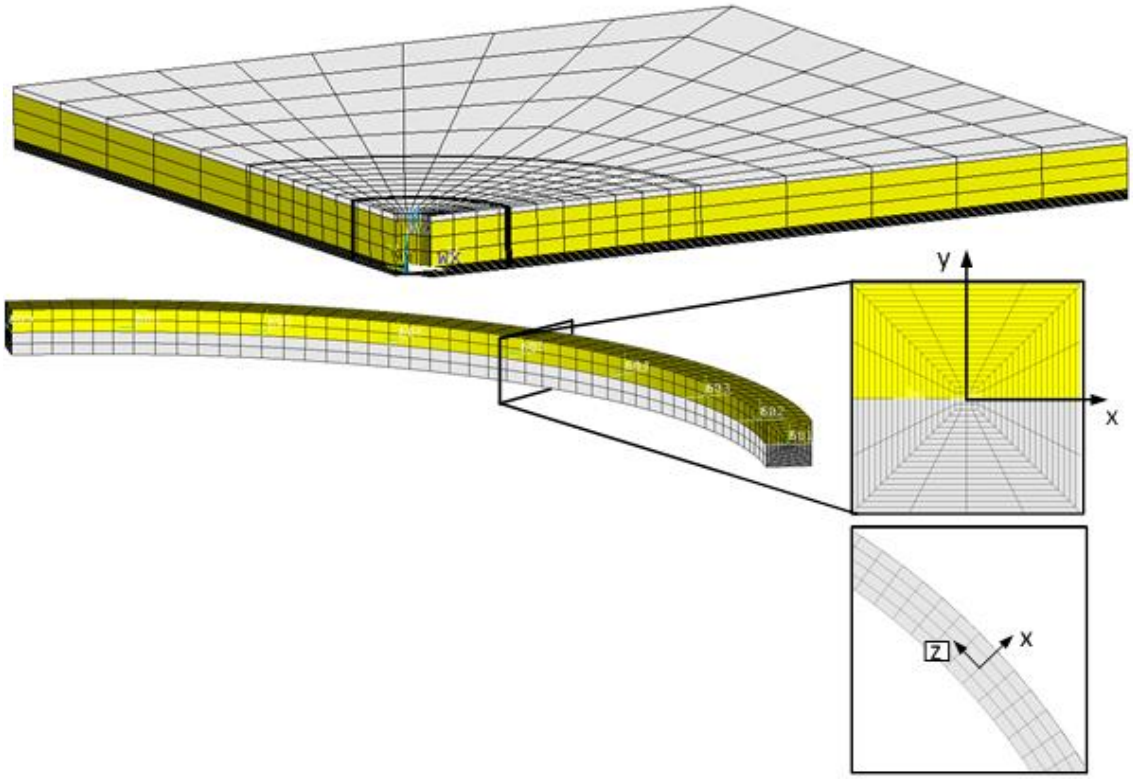

Figure 5. Global FE model of a sandwich panel specimen without a peel stopper (left), and FE sub-model and crack tip mesh along the crack front (right).

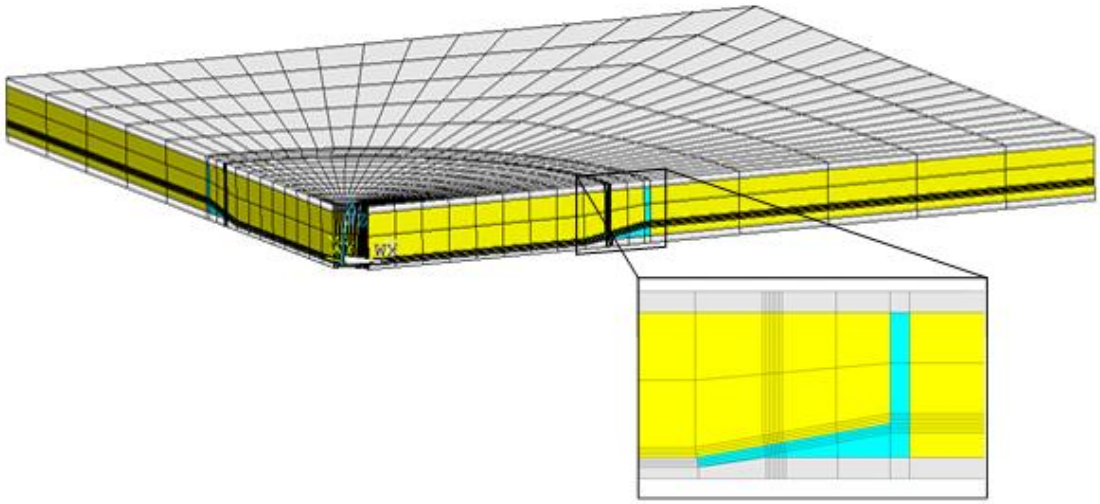

Figure 6. Global FE model of a sandwich panel specimen with an embedded peel stopper, and detailed meshing around the peel stopper, when the interface crack has been deflected.

3.1. Fatigue Crack growth analysis

As mentioned above the CSDE method [10-11] was used to derive the energy release rate and mode-mixity at the crack tip using relative displacements derived from the nodes in the crack tip wake from the FE model. For that purpose a dense crack tip mesh was used in the crack tip region and along the crack front of the debond, see Figure 5. Applying this mesh in the global FE model would result in very long computation times. Therefore, a sub-model containing only the crack tip elements was used for extracting the displacements, similar to applied in [13-15]. The sub-model routine is inherent in the ANSYS software, and works by transferring displacements from a coarse global model into a dense and more detailed sub-model in the form of boundary conditions. For this case, the detailed sub-model consisted only of the crack front and it was meshed by 20-node solid elements. The number of elements increased as the interface crack front propagated and increased in diameter. For the sake of simplicity, and also to save computation time, the sub-model was subject only to geometrically linear analyses. This was justified by the observation that the displacements and rotations at the crack tip are small, and thus there was no need for geometrically non-linear analysis on the sub-model scale. This simplification is important for the feasibility of the adopted approach, since the CSDE method is based on Linear Elastic Fracture Mechanics.

The crack front growth was controlled by nine independent control points along its length. Once the energy release rate and mode mixity were calculated they were used as input on the Paris law defining the crack growth rate in order to calculate the crack increment after one loading cycle. Each control point was then moved independently towards the individual crack growth direction. Once every control point position was updated, the new crack front was created.

After the displacements were extracted from the sub-model, they were used as input for the CSDE code that was implemented using the ANSYS APDL language. The energy release rate and mode-mixity equations used in the code are given by [10-11]:

$$\psi_K = \arctan\left(\sqrt{\frac{H_{22}}{H_{11}}}\frac{\delta_x}{\delta_y}\right) - \varepsilon\, ln\left(\frac{x}{h}\right) + \arctan(2\varepsilon) \tag{1}$$

$$G = \frac{\pi(1+4\varepsilon^2)}{8\,H_{11}|x|}\left(\frac{H_{11}}{H_{22}}\,\delta_y^2 + \delta_x^2\right) \tag{2}$$

where δ_x and δ_y are the crack shear and opening displacements of the crack tip nodes, ε is the oscillation index, and h is the characteristic length of the problem, which was set equal to the face-sheet thickness, i.e. *2* mm. H_{11} and H_{22} are the parameters that account for the anisotropic behaviour of both the face-sheet and the core, Table 5.

Every time the energy release rate and mode-mixity were calculated, the crack increment after one loading cycle was calculated by the use of Paris' Law [31]:

$$\frac{da}{dN} = m\,\Delta G^c \tag{3}$$

where a is the crack length, da is the crack length increment, and N and dN are the number of loading cycles and the increment in loading cycles, respectively. The parameters m and c are the fitting variables of the Paris' law curve. Finally ΔG represents the difference in energy release rate (ERR herinafter) between the maximum and minimum fatigue loads. In this study the ERR at the minimum fatigue load level was not specifically calculated. Instead it was considered to be equal to 10% of the ERR value corresponding to the maximum load, based on the load ratio $R=0.1$. The fitting parameters, m and c an were obtained from a previous study by Manca et. al. [32] in which fatigue crack growth tests were conducted for the face-sheet/core interface of sandwich MMB test specimens with the same face-sheet and core materials as in this study. The Paris law parameters for the PU/core interface were determined in [27] for similar crack growth conditions and are given in Table 5.

Table 5. CSDE and Paris' law parameters for the two interfaces.

	Face/core interface	PU/core interface

H_{11}	$1.68 \cdot 10^{-2} \left(\frac{1}{MPa}\right)$	$2.79 \cdot 10^{-2} \left(\frac{1}{MPa}\right)$
H_{22}	$1.56 \cdot 10^{-2} \left(\frac{1}{MPa}\right)$	$2.19 \cdot 10^{-2} \left(\frac{1}{MPa}\right)$
ε	$-7.066 \cdot 10^{-2}$	$-4.56 \cdot 10^{-2}$
h	2 mm	2 mm
c	$1.3758 \cdot 10^{-14}$	$0.9278 \cdot 10^{-14}$
m	4.55	4.486

After the crack increment was determined, the crack front was propagated by an increment corresponding to one loading cycle. Then the model was re-meshed and the analysis was repeated to derive the new interface crack front shape. To avoid repeating the process for all the loading cycles of the fatigue experiments, the Cycle Jump Technique [13-15] was applied. The technique requires at least three consecutive iterations of single cycle crack propagation simulations in order to predict the crack length after a larger number of non-simulated loading cycles. For further details on the CJT and the application in connection with fatigue propagation of a debond in a sandwich panel, see [13-15]. The fatigue crack growth simulation procedure outlined above enabled the seamless FE simulation of the entire fatigue experiments for both sandwich specimen types (i.e. with and without embedded peel stoppers).

4. RESULTS

The crack propagation process inside the sandwich panel specimens was difficult to monitor and evaluate during the actual experiments. Since the crack propagated inside the panels no in-situ visual confirmation of the debond front location was possible. Moreover, the DIC analyses required significant computation time during and after the experiments, before they could be used to evaluate the debond front location. As a result the only indication of the crack location during testing was the actuator piston displacement output measured at the peak loads by the test machine, see Figure 7. This is possible since the specimens compliance is directly linked to the debond radius. The displacements were recorded by the machine by measuring the actuator piston displacement under the constant load amplitude. . In this study, though, the displacements are not used for compliance calculations, but rather to demonstrate and evaluate the effect of the peel stopper. After the experiments were conducted, DIC was performed using the recorded images to obtain the displacement field of the facesheet around the panel centre.

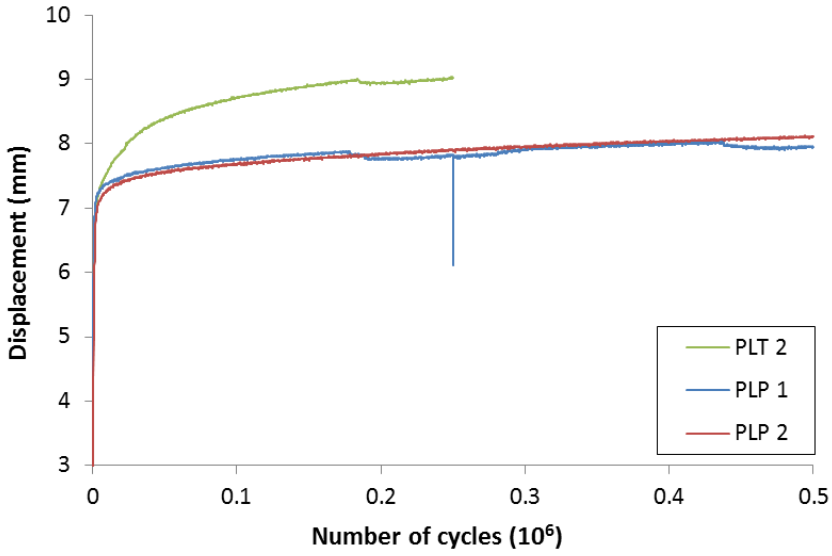

Figure 7. Measured piston displacement vs. number of cycles curves for the three fatigue tested sandwich specimens.

Figure 8 shows the vertical displacement field obtained from one of the tested panels (PLP1) containing a peel stopper next to the vertical displacement field obtained for the panel specimen without a peel stopper. The images correspond to the final stages of the two tests, i.e. 500,000 cycles for PLP1 (left), and 250,000 cycles for PLT2 (right). It is observed that the displacement field for specimen PLP1 with an embedded peel stopper is concentrated in the centre of the panel. In contrast to this, the displacement field is more uniform over the entire observed area for specimen PLT2 (without a peel stopper) indicating a much larger debonded area, which again shows that the interface crack has propagated more extensively for the sandwich panel without a peel stopper. It should be further noted that for the panel with an embedded peel stopper (PLP1), the number of loading cycles were double that of the loading cycles observed for the panel without a peel stopper.

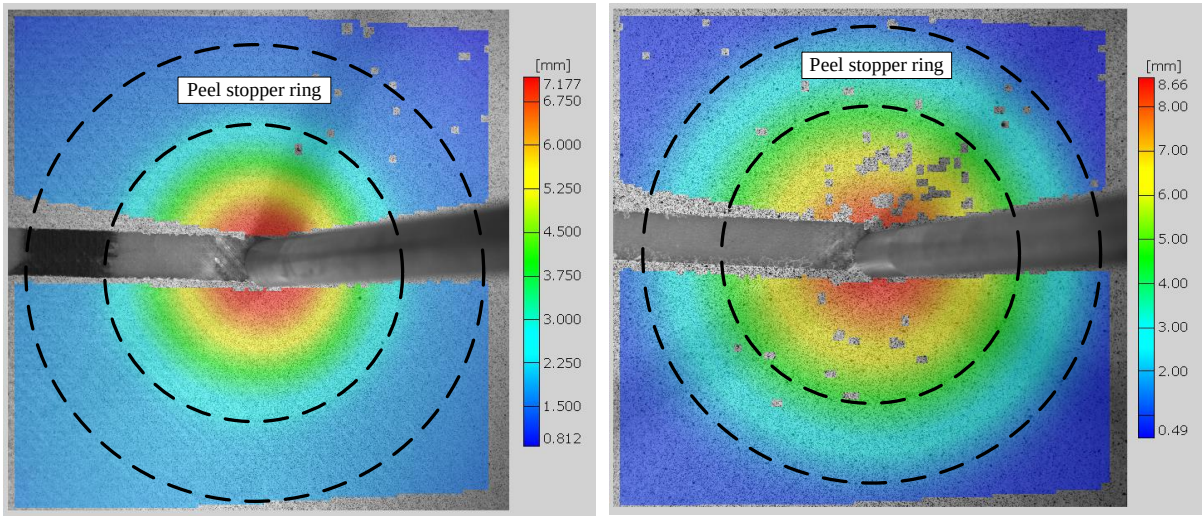

Figure 8. Sandwich panel specimens with (left – specimen PLP1) and without (right – specimen PLT2) embedded peel stoppers: DIC maps of vertical displacements at the end of the fatigue tests, corresponding to approx. 500,000 cycles for PLP1 (left) and approx. 250,000 cycles for PLT2 (right). The grey artifacts running horizontally through both images are the extension rod used for the application of the loading.

4.1. Tracking the crack

The post processed images from the digital cameras were used to extract the vertical displacement distribution along the axis of symmetry of the sandwich panel specimens. The displacement distributions were extracted from the DIC generated displacement data for all three sandwich panel specimens. These displacements were then used as input for a MatLab routine used for conducting numerical differentiation and smoothening to derive the first and second derivatives of the displacements along the x-symmetry axis (see Figure 1). The second derivative represents the curvature of the observed face-sheet. At the crack tip, an abrupt change of stiffness occurred due to the discontinuity caused by the debonded face-sheet. Since the face-sheet was responsible for carrying all of the transverse loading in the debonded area, a sudden increase of the curvature of the lower face-sheet was observed by DIC. Thus, it was hypothesized that the position of the crack tip corresponded to the local maximum of the second derivative of the displacement, as shown in, Figure 9. The vertical axes of the displacement and its two derivatives in Figure 9 have been "normalized" with respect to their peak value to demonstrate all three curves in one plot. Further, since the interface crack propagated axi-symmetrically away from the plate centre (see Figure 8), the crack front was traced and positioned by using just one point along the symmetry axis (x axis – see Figure 1) of the panel.

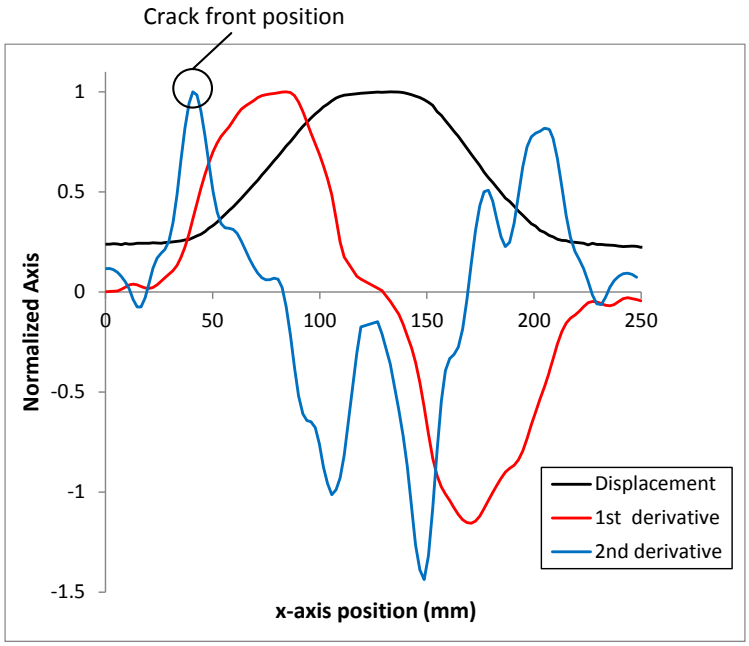

Figure 9. Normalised vertical displacement distribution for specimen PLP1 at 250,000 load cycles along the specimen x-axis (symmetry axis) derived from DIC, and the first and second derivatives of the displacement distribution.

The approach outlined above to track the crack front position is supported by the results of the FE analyses. Displacements from the nodes of the lower face-sheet were extracted from the FE model and used as input to the same MatLab algorithms. The algorithm was used to locate the crack tip, and this was then compared to the crack data input to the FE model. It was observed that the crack extension derived from the DIC data (Figure 9) consistently under-predicted the radial extension of the interface crack front by about 1-1.5 mm in comparison with the FE simulation results. The error could be partially due to the effect of the face-sheet thickness (2 mm) which was not taken into account in the MatLab algorithm. Since the differences observed between the FE simulated interface crack length and the experimentally derived results (shown in Figure 9) were consistent through all tests, the interface crack lengths derived using the DIC data were corrected by adding a 1 mm additional displacement (increase). The resulting "corrected" radial crack extension vs. number of loading cycles curve as obtained from the DIC calculated displacements is shown in Figure 10. An additional source of error could be the redirection of the crack front induced by the peel stopper. Therefore a loss of accuracy of the determination of the crack front position was therefore anticipated for crack lengths larger than 80 mm for the sandwich panel specimens with embedded peel stoppers. The reason for this is that when crack deflection occurred at the peel stopper tip, the interface crack would propagate towards the inner part of the core, thus increasing the distance from the lower face-sheet.

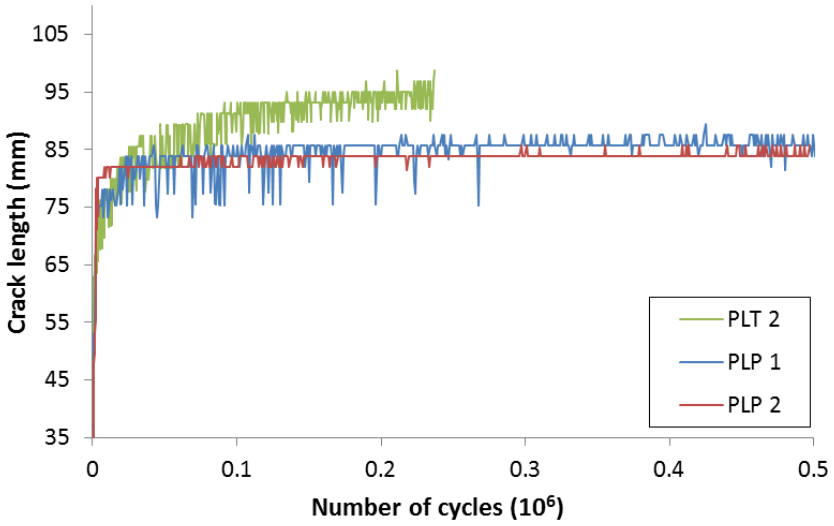

Figure 10. ”Corrected” interface crack length (radial direction) vs. number of load cycles.

4.2. Crack stopping effect

From Figures 7 and 10 it is observed that the interface crack growth was significantly influenced (delayed) by the presence of a peel stopper. To verify the experimental observations, the sandwich panel specimens were cut up after the tests to inspect the crack paths. Figure 11 shows two section cuts from specimens PLP2 (below - with peel stopper) and PLT2 (top - without peel stopper). The two cut sections are aligned so that the loading points of the two specimens are coinciding. For specimen PLT1 is observed that no crack deflection occurred, while it is observed that crack deflection occurred for specimen PLP2. The interface cracks in both specimens were measured and compared with the crack lengths extracted from the DIC data. For both cases the DIC measurements were very close to the crack lengths observed from the cut specimens. The crack in the panel without a peel stopper (PLT2) propagated up to about 100 mm during 250,000 loading cycles, thus exceeding the peel stopper boundaries (96 mm). For the panel with an embedded peel stopper (PLP2) the interface crack was measured to be about 87 mm long after a total of 500,000 loading cycles. Thus, it is concluded that the peel stoppers were successful in confining the propagating interface crack. From the post-mortem specimen images and crack lengths extracted from the DIC measurements it is observed that the interface crack propagation rate was slowed down considerably after crack deflection occurred for specimen PLP2.

Figure 11. Post mortem sections of sandwich panel specimens PLT2 (above – no peel stopper) and PLP2 (below - with embedded peel stopper).

In the next section the above observations will be further explained by examining the ERR and mode-mixity evolution at the crack tip after crack deflection occurred in the panels with embedded peel stoppers. Since the interface cracks did not reach the limits of the allowable growth area, i.e. peel stopper outer boundary, it was not possible to achieve complete crack arrest during the experiments. This suggests that the increase of the fatigue life of the sandwich panel with embedded peel stoppers is not fully demonstrated by the conducted experiments. Moreover, as described in previous research [27, 28], most of the load cycles endured while the crack is arrested occurs after the crack has reached the boundary of the area confined by the peel stopper

5. NUMERICAL SIMULATION RESULTS

The predicted loading point (vertical) displacement and the interface crack length evolution during the fatigue testing are shown in Figures 12 and 13 for sandwich panels with embedded peel stoppers and without peel stoppers. The crack length data are extracted from the FE model at the location of the crack front nodal points parallel to the x-axis (see Figure 1). The experimentally determined values are also shown in the figures. Figure 12 shows that the FE modelling was able to capture the initial steep rise in displacement as well as the plateau that was reached at the final stages of the fatigue experiment. In a similar manner it is observed from Figure 13 that the FE modelling accurately predicted the crack propagation rate during the entire fatigue experiment for the specimens with embedded peel stoppers. However, for the specimen without peel stoppers the FE model over-predicts the crack growth. This can be attributed to the large geometrically non-linear effects that are not captured correctly at very large crack lengths (radial crack extensions). Despite the discrepancies found for the specimen without an embedded peel stopper, the results demonstrate that the developed 3D FE modelling approach was capable of accurately predicting the overall fatigue behaviour of the sandwich specimens with embedded peel stoppers.

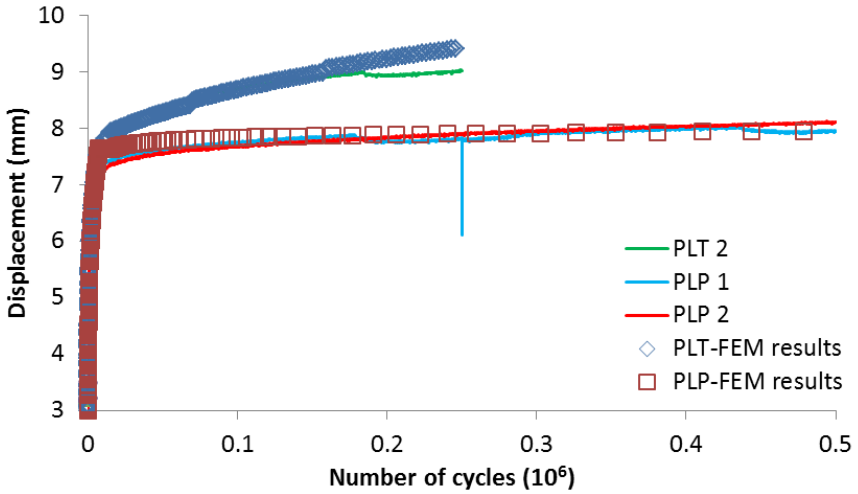

Figure 12. Central displacement for specimens PLP1, PLP2 (with embedded peel stoppers) and PLT2 (without peel stopper) vs. number of loading cycles; FE model predictions and experimental results (piston displacement of test machine).

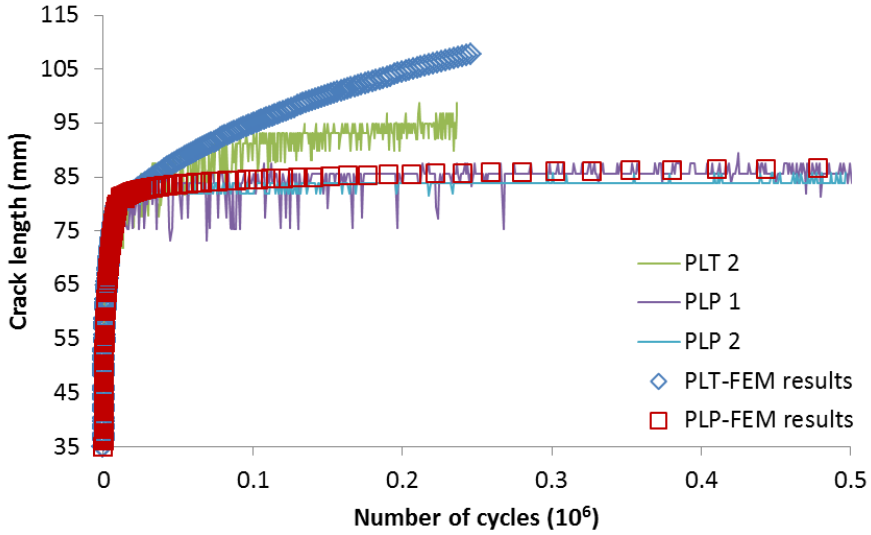

Figure 13. Interface crack length evolution vs. number of loading cycles; FE predictions and experimental results for specimens PLP1, PLP2 (with embedded peel stoppers) and PLT2 (without peel stopper).

The fatigue testing was limited to 500,000 loading cycles (for specimens PLP1 and PLP2 with embedded peel stoppers). To develop a further understanding of the effect and performance of the embedded peel stoppers, the FE simulation of the fatigue process together with the fatigue crack propagation algorithm has been used to extrapolate beyond 500,000 loading cycles. Figures 14 and 15 show the predicted ERR and mode-mixity against number of cycles and crack length, respectively. The fatigue experiments were simulated up to 2 million loading cycles, which is considered to be a realistic expected fatigue life for many foam cored composite sandwich structures.

From Figure 14 and 15 it is observed that the ERR drops significantly after the propagating interface crack has been deflected by the peel stopper, whereas the mode-mixity increases. Figure 14 shows that the ERR reaches a plateau which is associated with a drastic decrease in crack growth rate, when the propagating interface crack reaches the peel stopper (corresponding to approximately 25,000 cycles and a crack length of 80 mm). It is further seen that the mode-mixity increases continuously at a very low rate throughout the fatigue process. Figure 15 provides further information

about the behaviour of the sandwich panel specimens in the earlier stages of the fatigue process. Thus, it is observed that the ERR is very high for small interface crack lengths, and that it decreases considerably as the crack propagates. This explains the very high propagation rate observed at the beginning of the fatigue process, as well as the crack arresting effect when the radial extension of the crack (the crack length) becomes larger. It is further observed that the mode-mixity increases slightly during crack propagation in the face-sheet/core interface, and that the mode-mixity increases significantly, when the interface crack deflects into the core at the peel stopper tip. This can be explained by the change in the angle of crack propagation, as the interface crack is forced to propagate at an angle of 10^{o} relative to the face-sheet. This increases the shear component (mode II) of the propagating crack front, since the crack naturally tends to propagate towards the lower face-sheet under such loading conditions.

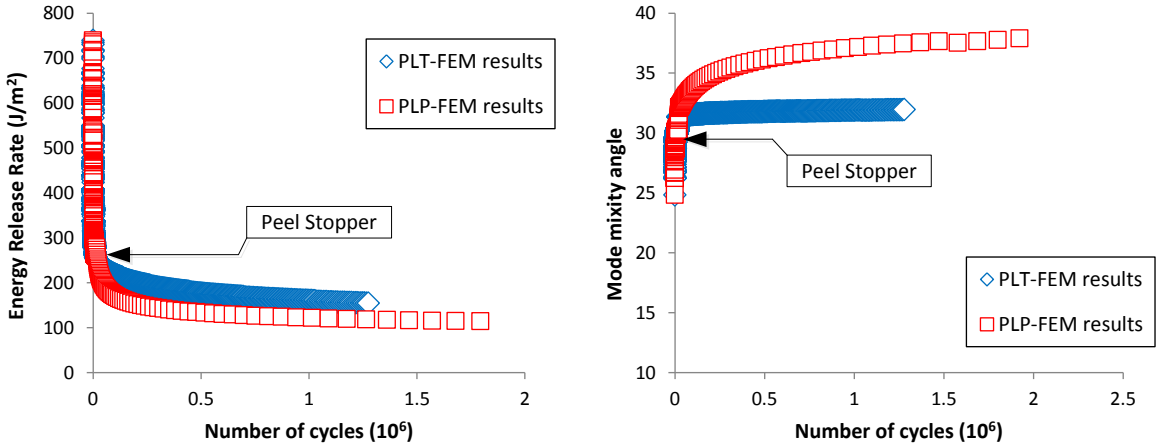

Figure 14. FE simulation of the fatigue process in the sandwich panel specimens with (PLP) and without peel stoppers (PLT): ERR and mode-mixity vs. number of loading cycles for up to 2×10^{6} cycles

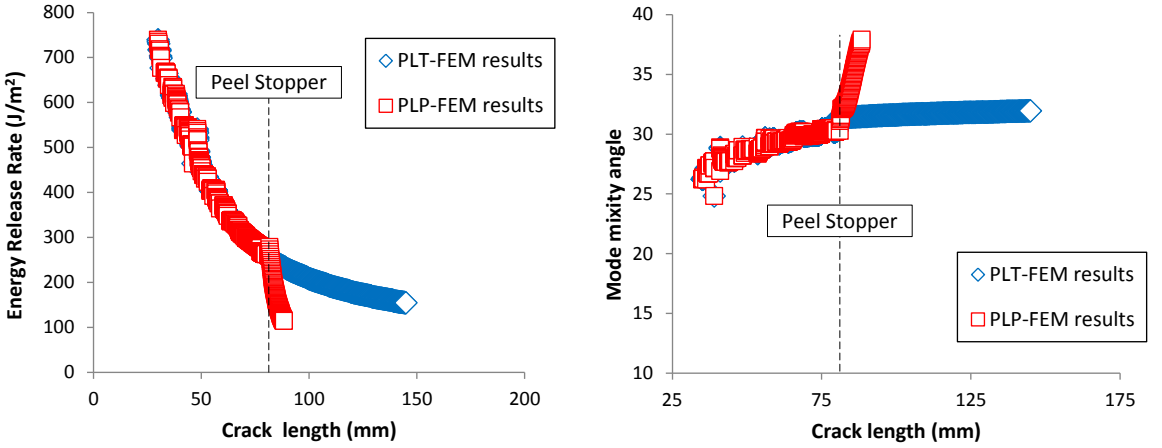

Figure 15. FE simulation of the fatigue process in the sandwich panel specimens with (PLP) and without peel stoppers (PLT): ERR and mode mixity vs. crack length.

From Figure 14 and 15 it is further seen that the crack growth conditions, imposed at the crack front after it has been deflected by the peel stopper, are such that the propagating crack is arrested inside the peel stopper. Moreover, the FE simulations predict that the propagating crack will not reach the physical boundary (radius of 98 mm) of the peel stopper even after 2 million cycles, Figure 15. Previous studies [27,28] have shown that most of the time (or loading cycles) to crack arrest is endured while the crack tip is located near the physical boundary of the peel stopper (referred to as the arrest point). In the research conducted in [27, 28] concerning sandwich beams with embedded peel stoppers, it

was observed that at this point the crack propagation stopped completely, and that a new crack was initiated on the opposite side (or behind) of the peel stopper. This behaviour (i.e. initiation of a new crack behind the peel stopper) was not observed in this study on sandwich panels (plate structures) with embedded peel stoppers, thus indicating that the potential advantage of peel stoppers (in terms of increased fatigue life and improved damage tolerance) is even higher for sandwich panels than for sandwich beams.

6. DISCUSSION

Special crack stopping elements or devices, referred to as peel stoppers, have been introduced into composite face-sheet and foam cored sandwich panels that were tested under fatigue loading conditions. The main goal of the study was to demonstrate the feasibility and to quantify the effects on the fatigue life of such peel stoppers. The proposed peel stopper concept has previously been investigated and tested in foam cored sandwich beams, and it was shown that the fatigue life was improved considerably [27, 28].

The fatigue loading conditions were introduced into the sandwich panels through a central point force applied through a rigid insert. The loading and sandwich specimen layout were chosen and designed so as to propagate an initial face-sheet/core interface crack front away from the centre of a square sandwich panel and towards the panel edges. The damage evolution (interface crack propagation) was recorded using DIC on the loaded (and debonded) face-sheet, and the displacement of the loading point (assumed to be equal to the piston displacement of the test machine) was used to capture the evolution of the sandwich panel stiffness through the fatigue process.

The experimental results showed that for the sandwich panels with embedded peel stoppers the propagating face-sheet/core interface crack was deflected and re-directed into the core structure. As a result the propagating crack was decelerated considerably, and it was arrested completely inside the peel stopper. The testing of a foam cored sandwich panel without peel stoppers, and subjected to identical fatigue loading and boundary conditions, displayed a much faster interface crack growth and importantly no crack deflection occurred. The crack also slowed down and was arrested in the sandwich panel without an embedded peel stopper. This was anticipated as the crack tip stresses reduces with the radial distance from the load application point for the chosen panel test configuration. No quantitative criterion regarding the desired and/or expected performance of the sandwich panels with embedded peel stoppers was specified a priori. Because of this, and since the panel specimens were not completely delaminated after the fatigue testing, a quantitative analysis on the performance of the sandwich panels with embedded peel stoppers was not conducted. However, it is clear from the obtained results that the inclusion of peel stoppers in foam cored sandwich panels significantly improves the resistance to interface crack propagation, and thereby also the damage tolerance.

To further substantiate and validate the findings of the conducted fatigue experiments, a numerical study was conducted to extract fatigue crack growth data for the face-sheet/core interface crack in the tested sandwich panel specimens. To achieve this, a finite element based analysis procedure was developed to simulate the complete fatigue process. The numerical predictions are in excellent agreement with the obtained experimental results when the crack radius extends within the peel stopper limits. For very large crack lengths outside of the peel stopper region the numerical and experimental observations begin to diverge considerably. Moreover, the numerical results explain the deceleration of crack growth when the propagating interface crack is deflected by the peel stopper. It is shown that the energy release rate (ERR) decreases considerably when the crack is deflected away from the face-sheet/core interface. The analysis results further show that the mode II component of the crack tip stress field increases significantly, especially when the crack reaches deep into the core structure following the peel stopper contour.

7. CONCLUSIONS

The proposed crack stopping device (or concept) has significant potential for practical use in critical load carrying sandwich structures, as it offers significant improvement of the damage tolerance. More specifically, the fatigue life of sandwich structures with embedded peel stoppers (as proposed) will be significantly improved, and the vision is that load carrying sandwich structures with embedded peel stoppers may be used in service even after face-sheet/core damage (debonds/delamination) has been detected inside. The proposed peel stopper concept enables the pre-specification of physical boundaries or borders through the embedding of a grid-work or system of peel stoppers, that

will effectively confine debond/delamination damage to small pre-selected areas in the sandwich structural layout. Depending on the particular application and the desired limitations, internal interface damage propagation or global stiffness reduction could potentially be effectively controlled.

ACKNOWLDGEMENTS:

The work was sponsored by the Danish Council for Independent Research | Technology & Production Sciences (FTP) under the research grant "Enhanced Performance of Sandwich Structures by Improved Damage Tolerance" (SANTOL) (Grant 10082020). The Divinycell H100 material used in this study was provided for free by DIAB A/S. The work has been conducted in collaboration with and co-sponsored by the Technical University of Denmark, Aalborg University, Denmark, the University of Southampton, UK, Siemens Wind Power A/S, Denmark, and LM Wind Power Blades A/S, Denmark.

REFERENCES

[1] Zenkert, D: An introduction to sandwich construction, London: Chameleon Press Ltd (1995)

[2] Shenoi, R.A, Groves, A, Rajapaske, Y.D.S.: Theory and Applications of Sandwich Structures, University of Southampton RGSE, ISBN-13: 978-0854328253 (2005)

[3] Erdogan, F.: Bonded dissimilar materials containing cracks parallel to the interface, Engineering Fracture Mechanics, 3:231-240 (1971)

[4] Dundurs, J.: Edge-bonded dissimilar orthogonal elastic wedges. J.Appl.Mech, 36:650-652 (1969)

[5] Hutchinson, J.W., Suo, Z.: Mixed Mode Cracking in Layered Materials, Advances in Applied Mechanics, 29:63-191 (1992)

[6] Suo, Z.: Singularities, interfaces and cracks in dissimilar media. Proc. R. Sot. Land, A427:331-358 (1990)

[7] He M., Hutchinson J.W.: Kinking of a Crack Out of an Interface. ASME. J. Appl. Mech. 56:270-278 (1989)

[8] Wang, T. C.: Kinking of an interface crack between two dissimilar anisotropic elastic solids. International Journal of Solids and Structures, 31:629–641 (1994)

[9] Krueger, R.: Virtual Crack Closure Technique: History, Approach and Applications," Applied Mechanics Reviews, 57:109-143 (2004)

[10] Jolma, P., Segercrantz, S., & Berggreen, C.: Ultimate Failure of Debond Damaged Sandwich Panels Loaded with Lateral Pressure: An Experimental and Fracture Mechanics Study. *Journal of Sandwich Structures and Materials*, *9*(2), 167-196 (2007)

[11] Berggreen, C. C., Simonsen, B. C., & Borum, K. K.: Experimental and Numerical Study of Interface Crack Propagation in Foam Cored Sandwich Beams. *Journal of Composite Materials, 41*(4), 493-520 (2007)

[12] Bak, B. L. V., Turon, A., Lindgaard, E., Lund, E.: A simulation method for High-Cycle Fatigue-Driven delamination using a cohesive zone model. Int. J. Numer. Meth. Engng (2015)

[13] Moslemian, R., Karlsson, A. M., Berggreen, C.: Accelerated fatigue crack growth simulation in a bimaterial interface. International Journal of Fatigue, 33:1526–1532 (2011)

[14] Moslemian, R., Berggreen, C., & Karlsson, A. M.: Application of a Cycle Jump Technique for Acceleration of Fatigue Crack Growth Simulation. In *Proceedings — NAFEMS Nordic Seminar: Simulating Composite Materials and Structures*, (2010)

[15] Moslemian, R., Berggreen, C., Quispitupa, A., & Hayman, B.: Damage assessment of compression loaded debond damaged sandwich panels. In G. Ravichandran (Ed.), *ICSS 9* (2010)

[16] Rinker, M., Zahlen, P. C., John, M., Schäuble, R.: Investigation of sandwich crack stop elements under fatigue loading. Journal of Sandwich Structures and Materials, 14:55–73 (2012)

[17] Hirose, Y., Matsubara, G., Hojo, M., Matsuda, H., Inamura, F.: Evaluation of modified crack arrester by fracture toughness tests under mode I type and mode II type loading for foam core sandwich panel. In: Proc. US-Japan conference on composite materials 2008, Tokyo, Japan (2008)

[18] Hirose, Y., Matsuda, H., Matsubara, G., Hojo, M., Inamura, F.: Proposal of the concept of splice-type arrester for foam core sandwich panels. Composites Part A: Applied Science and Manufacturing, 43:1318–1325 (2012)

[19] Jakobsen, J., Bozhevolnaya, E., Thomsen, O.T.: New peel stopper concept for sandwich structures. Compos Sci Technol, 67:3378–85 (2007)

[20] Jakobsen, J., Andreasen, J.H., Bozhevolnaya, E.: Crack kinking of a delamination at an inclined core junction interface in a sandwich beam. Eng Fract Mech, 75(16):4759–73 (2008)

[21] Bozhevolnaya, E, Jakobsen, J & Thomsen, O.: Fatigue Performance of Sandwich Beams With Peel Stoppers, 45:349-357 (2009)

[22] Bozhevolnaya, E., Jakobsen. J., Thomsen, O.T.: Performance of sandwich panels with peel stoppers, strain. Int J Exp Mech, 45:349–57 (2009)

[23] Jakobsen, J., Thomsen, O.T., Andreasen, J.H., Bozhevolnaya, E.: Crack deflection analyses of different peel stopper design for sandwich structure. Compos SciTechnol, 69:870–5 (2009)

[24] Jakobsen, J, Andreasen JH, Thomsen OT.: Crack deflection by core junctions in sandwich structures. Eng Fract Mech 76(14):2135–47 (2009)

[25] Jakobsen, J., Johannes, M., Bozhevolnaya, E.: Failure prediction of in-plane loaded sandwich beams with core junctions. Composite Structures 82 (2), 194-200 (2008)

[26] Wang, W., Martakos, G., Dulieu-Barton, J. M., Andreasen, J. H., Thomsen, O. T.: Fracture behaviour at tri-material junctions of crack stoppers in sandwich structures. Composite Structures, 133, 818-833 (2015)

[27] Martakos, G., Andreasen J.H., Berggreen C., Thomsen O.T.: Experimental Investigation of Interfacial Crack Arrest in Sandwich Beams Subjected to Fatigue Loading using a Novel Crack Arresting Device. Submitted for publication.

[28] Martakos, G., Andreasen J.H., Berggreen C., Thomsen O.T.: Interfacial Crack Arrest in Sandwich Beams Subjected to Fatigue Loading using a Novel Crack Arresting Device - Numerical modelling. Submitted for publication.

[29] DIAB. Divinycell H-Grade Technical data, Laholm (Sweeden), 2014. (http://www.diabgroup.com).

[30] ANSYS® Academic Research, Release 15.0

[31] Paris, P., Erdogan, F.: A critical analysis of crack propagation laws, J Basic Engng Trans ASME Ser D, 85:528–534 (1963)

[32] Manca, M., Berggreen, C., Carlsson, L. A.: G-control fatigue testing for cyclic crack propagation in composite structures. Engineering Fracture Mechanics (2015)